Biosensors and Bioelectronics 40 (2013) 38–44

Contents lists available at SciVerse ScienceDirect

Biosensors and Bioelectronics

journal homepage: www.elsevier.com/locate/bios

Label-free, needle-type biosensor for continuous glucose monitoring based on competitive binding

Sung-Ho Paek [a], Il-Hoon Cho [a], Dong-Hyung Kim [a], Jin-Woo Jeon [a], Guei-Sam Lim [a,b], Se-Hwan Paek [a,c,*]

[a] Department of Bio-Microsystem Technology, Korea University, 1, 5-ka, Anam-dong, Seongbuk-gu, Seoul 136-701, Republic of Korea
[b] Healthcare Group, Emerging Technology Lab., LG Electronics Advanced Research Institute, 16 Woomyeon-dong, Seocho-gu, Seoul 137-724, Republic of Korea
[c] Department of Biotechnology and Bioinformatics, Korea University, Jochiwon, Choongnam 339-800, Republic of Korea

ARTICLE INFO

Available online 7 June 2012

Keywords:
Continuous glucose monitoring
Concanavalin A as glucose binder
Needle-type implantable sensor
Rate-limiting factors
Label-free signal detection

ABSTRACT

With the goal of developing a method for the continuous monitoring of blood glucose, an implantable sensor was developed by placing an optical fiber probe within the internal hollow space of a syringe needle. A glucose binder, concanavalin A (Con A), was immobilized on the probe tip and a protein (e.g., bovine serum albumin) chemically coupled with a sugar ligand (e.g., mannose) was loaded as a solution inside of the needle, which were then closed using a semi-permeable membrane. Upon immersion in the glucose sample, small molecules were able to freely pass through the membrane and compete with the ligand conjugate for Con A binding. This changed the molecular layer thickness on the probe surfaces depending on the glucose concentration, which shifted the wavelength of the guided light along the fiber. Such interference in the wavelength pattern was measured using a commercial sensor system, Octet, without employing a label. Using this analytical approach, two major steps controlling the performance of glucose detection were overcome: permeation of glucose (optimum with 50 nm-porous polycarbonate membrane under the experimental conditioned used) and molecular diffusion of the ligand conjugate within the sensor compartment (19 gauge-needle, offering minimal demensions for the probe). Under optimal conditions, the sensor was able to monitor glucose fluctuations, even in serum medium, with a response time of less than 15 min in a range 10–500 mg/dL. This, however, could be further shortened down to about 5 min in principle by miniaturizing the sensor dimensions.

1. Introduction

Diabetes mellitus is a disease that can be managed by controlling blood glucose concentrations (Paek et al., 2011). However, disease management depends on closed-loop insulin delivery (Hovorka, 2011), which can be achieved by using a continuous glucose monitoring (CGM) system that can directly signal to a drug reservoir (Leney and Tavaré, 2009). However, such a CGM cannot be developed using conventional enzyme sensors, which are based on a finger-prick (Steiner et al., 2011), because of limitation in the frequency of blood draws (Dunn et al., 2004). Modified versions of enzyme sensors that can be attached to the body have been developed for CGM, which are currently available in hospitals to monitor glucose concentrations over several consecutive days (Wei et al., 2010). However, there are several limitations to this approach; the sensor needs to be calibrated several times a day, body fluid is continuously consumed and only discrete measurements over a predetermined time interval can be obtained (Boss et al., 2011).

Several of the drawbacks associated with current CGM systems can be addressed by introducing a non-catalytic sensor, which utilizes a glucose binder, such as organic boronic acids (Li et al., 2008), concanavalin A (Boss et al., 2011), glucose-binding apoenzymes (Chaudhary et al., 2009), glucose-binding proteins (Jin et al., 2011), and glucose-binding monoclonal antibodies (Paek et al., 2011). They all interact with glucose in a reversible reaction, i.e., variable complex formations depending on the analyte concentration in sample, which can be exploited for true continuous monitoring. Optical detection methods have been widely applied to quantitatively detect binding complexes based mainly on fluorescence inhibition due to either competitive binding or structural conformation changes of the binder upon interaction (Steiner et al., 2011). Such sensors require a label, such as a chemical, biological fluorophores and enzymes to produce a signal that can be detected by a physical transducer. Thus, the performance of the sensor is dependent on several other factors related to the stability of the label and interference of signal transmission to the detector (Steiner et al., 2011).

A label-free approach may be an alternative means to measure glucose binding directly to the binder or by competition (Paek et al., 2011). Among previously investigated CGM systems, a

* Corresponding author. Tel.: +82 2 3290 3438; fax: +82 2 927 2797.
E-mail address: shpaek@korea.ac.kr (S.-H. Paek).

0956-5663/$ - see front matter © 2012 Elsevier B.V. All rights reserved.
http://dx.doi.org/10.1016/j.bios.2012.05.038

change of osmotic pressure (Krushinitskaya et al., 2011), viscosity (Steiner et al., 2011), or surface mass (Mori et al., 2009) according to the interaction was measured using the appropriate detectors. These systems are not only free from the burdens associated with labeling, but are also more suitable for analyzing samples that do not require a high sensitivity, which is not the case for CGM. Recently, optical sensing via a fiber sensor was developed to measure a shift in the wavelength of a guided light by interference due to binding on surfaces (Paek et al., 2011). Such fiber sensor technology could be particularly interesting because the optical signal at the local surfaces can be transmitted to a spatially separated detection device without interference. Even more, the detector can potentially be miniaturized for use on body skin, while not being affected by electromagnetic fields (Wang, 2007).

In this study, we developed a bio-layer interferometric glucose sensor by placing an optical fiber within a distal piece of a syringe needle, which could be readily implanted into the body. Con A, the glucose- and mannose-specific lectin, was used as a binder for glucose, which can further be applied for the development of a closed-loop insulin delivery system (Hovorka, 2011). Since Con A has been shown to be associated with a variety of toxicological effects (Li et al., 2008), the tip of the fiber sensor was coated with Con A and a sugar-protein conjugate in solution was placed in the vacant space of the needle, which was closed by a semi-permeable membrane. Upon immersion in medium, the optical signal would change due to the competitive binding for Con A between glucose and the ligand conjugate. This potential analytical concept was examined using a commercial, label-free detection system, referred to as Octet, and the rate-liming factors controlling the performance were determined.

2. Materials and methods

2.1. Materials

All reagents used in this study were of analytical grade and listed in Supplementary Information.

2.2. Preparation of analytical Components

Two polysaccharides, mannose and dextran (molecular weight (MW) 10 K), were chemically coupled to bovine serum albumin (BSA) by using the divinyl sulfone (DVS) cross-linking method (Paek et al., 2011). After separation of the unreacted sugars, the final products were analyzed by sodium dodecyl sulfate-polyacrylamide gel electrophoresis (SDS-PAGE). The products were also characterized by binding them to Con A-immobilized sensors, which were installed within a label-free sensor system, Octet Red (ForteBio, San Francisco, CA). To develop an experimental model for CGM, the analytical components were rearranged to establish four different models (A-1 and 2, and B-1 and 2), which provided variable response times and signal levels. The binding reactions of association and dissociation were observed under the same physical conditions. For model A-1, the effect of glucose binding on the sensor performance was further examined. Experimental details were presented in Supplementary Information.

2.3. Construction of needle-type sensor with semi-permeable membrane

Syringe needles were cut into a length of 6.5 mm and 4.5 mm from the tip for 17 gauge and 19 gauge needles, respectively, and a semi-permeable membrane was then attached onto the diagonal end of the surfaces using medical grade epoxy. After washing, the mannose conjugate was loaded into the hallow space and the Con A-immobilized sensor was then inserted through the top opening. Finally, the annulus space between the sensor and the needle was filled with mineral oil and subsequently blocked with silicon glue. Experimental conditions were presented in detail in Supplementary Information.

2.4. Determination of rate-controlling factors

We compared the performances of the sensors employing different semi-permeable membranes: regenerated cellulose membranes (MW cut-off (MWCO) 12 K) and polycarbonate membranes with 30 to 80 nm pore sizes. The tests were carried out using the label-free sensor system. The internal sensor volume was also varied by employing different needle sizes (17 and 19 gauges) and, in this case, 50 nm-porous polycarbonate membrane was installed. Finally, using a 19 gauge needle, the effect of the pore size of the semi-permeable membrane (50 or 80 nm) on the retention of the conjugate was tested. Detailed protocols were shown in Supplementary Information.

2.5. Assessment of sensor performances

Under optimal conditions, the dynamic range of glucose detection and response time of the needle-type sensor were tested. To this end, the BSA-mannose conjugate (3 mg/mL) was loaded into the 19 gauge needle, which was closed with a 50 nm-porous polycarbonate semi-permeable membrane. After assembly, the needle-type sensor was used to measure glucose levels in standard samples ranging from 10 to 500 mg/dL. The background was monitored using the same sensor in solution not containing the sugar conjugate. The differential signal was produced using Data Analysis 7.0 program. For a close simulation of clinical testing, the needle-type sensor was also applied to measure glucose spiked in human serum. Supplementary Information can be referred for details.

3. Results and discussion

3.1. Model sensor system

In this study, a novel CGM system was developed and was based on competitive binding between glucose and a ligand-substituted protein conjugate for Con A on sensor surfaces. Since the recycling of the components should be a precondition for continuous measurements, they were confined within a compartment (e.g., hollow space of syringe needle) that was isolated by a semi-permeable membrane from the sample medium (Fig. 1, the left). The analyte, glucose, is a small molecule that can freely pass through the membrane. Therefore, the glucose concentration was the only variable to be determined, while other components, Con A and the conjugate, remained constant so that the competition on the sensor could be changed by the analyte level in the sample. A commercial product, Octet Red, was used as the label-free sensor device, where the molecular interactions on the sensor surfaces cause a change in the interference pattern of white light reflected from the immobilized layer relatively to that from an internal reference layer. This results in a wavelength shift, which can be used as a direct measure of the change in thickness of the sensor layer.

We developed a competitive binding reaction system where Con A, which was used as the binder, was immobilized on the sensor tip surfaces and a carrier protein (e.g., BSA) chemically substituted with mannose, which was used as the ligand, was located in the aqueous solution. Other configurations of the

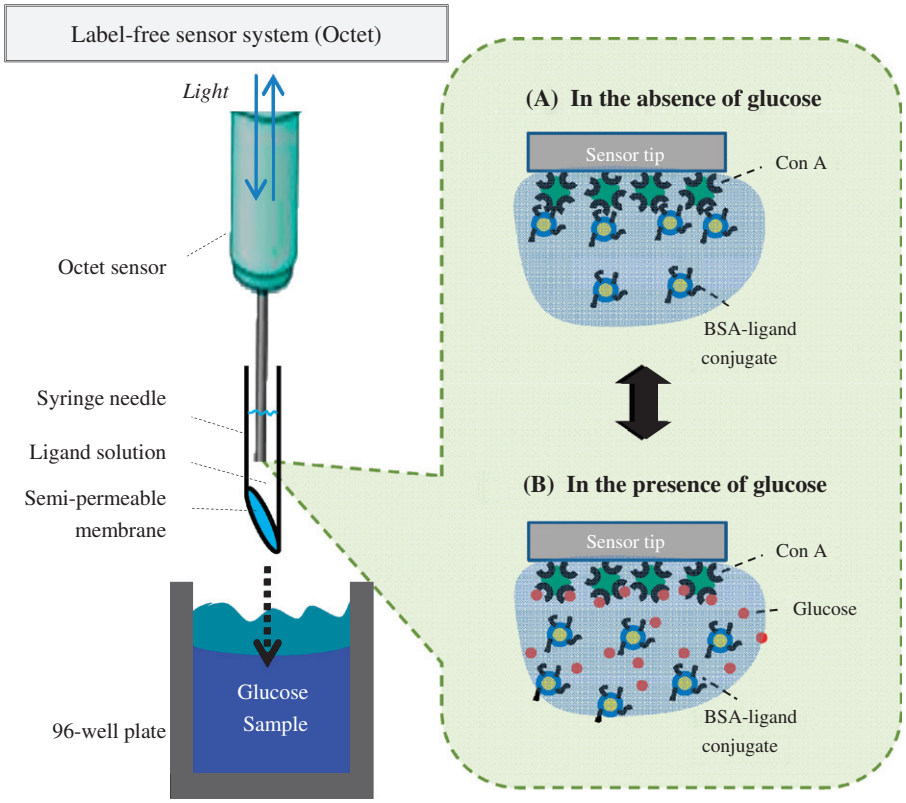

Fig. 1. A label-free sensor system for CGM using Con A as binder. Con A immobilized on the sensor tip and a ligand species in solution were confined within a syringe needle by a semi-permeable membrane, which was then dipped into a sample well placed within the label sensor system (e.g., Octet Red, the left). The binding components retained within the compartment were recycled for CGM. In the absence of glucose (A), the ligand reacted with the binder, which increased the sensor signal. In the presence of glucose (B), upon influx through the membrane, the analyte competitively bound to Con A and dissociated the ligand, which decreased the signal.

components were also feasible, which will be described in further detail below. In the absence of glucose, the ligand was the sole component that bound to the binder. Such binding increased the signal from the label-free sensor system, until the reaction reached equilibrium (Fig. 1A). In the presence of excess glucose, it permeates across the membrane and competes with the ligand for binding to Con A. This competition eventually dissociates the ligand from the binding sites, causing an abrupt decrease in the signal from the sensor to a minimum level (1B). These two extreme cases regarding the binding reactions are reversible and are based on the changes in glucose concentration in the sample.

Con A has been used in previous studies as a sugar-binding protein to monitor blood glucose levels and has been incorporated into various sensor systems (Boss et al., 2011). In this study, we utilized Con A in combination with the label-free optical sensor device, which could potentially be miniaturized by manufacturing an optical fiber (Ma and Wang, 2010) that could be inserted inside an implantable syringe needle. To eventually use it for CGM, the biosensor performance must satisfy clinical requirements, including a dynamic range, response time, reproducibility, ease of calibration, biocompatibility, and so on. Even at the initial stage of development, these factors should be considered, particularly, detection of glucose in a clinical range and rapid response time, which must be sufficient to follow analyte fluctuations in vivo.

3.2. Definition of performance-controlling variables

We prepared the major components, and optimized the factors controlling the response time and detection range, including the synthesis of the ligand-coupled carrier protein, rearrangement of component species, and selection of a suitable semi-permeable membrane and syringe needle.

3.2.1. Chemical substitution of carrier protein with ligand

Carbohydrates were conjugated to the carrier protein, BSA, so that the ligand component was retained within the sensor compartment, which was enclosed by a semi-permeable membrane. Dextran, which has a MW of 10 K and mannose, which can bind to Con A, were chosen as the sugar ligands (Ohyama et al., 1985). The ligands were individually conjugated to the protein via cross-linking using DVS (Supplementary Fig. 1A), which allows for covalent coupling between the hydroxyl group of the sugar and amino moiety of the protein under different pH conditions (Liu et al., 2002). After conjugation, the mean molecular size was shifted from the monomer to a dimension much higher than 170 kDa. Such large conjugate would be sufficiently retained within the sensor compartment by the semi-permeable membrane with a high MWCO. Under such conditions, glucose permeation across the membrane will be accelerated and its effect on the sensor performance will be minimal.

After fractionation, each sugar-protein conjugates were functionally characterized by reacting them with Con A immobilized on the sensor surfaces (Supplementary Fig. 1B). Con A consists of four subunits, each of which contains a sugar binding site and two metal binding sites for Mn^{2+} and Ca^{2+} (Boss et al., 2011). The protein reacts strongly with mannose and a variety of other sugar components with different binding forces (Mandal et al., 1994). In the binding experiments, Con A was fixed on distinct optical fiber sensor tips of a label-free sensor system, Octet Red, which can monitor changes in the thickness of the molecular layer formed on the sensor tip surfaces (Paek et al., 2011). Both of the

conjugates appeared to bind to Con A, where the mannose conjugate showed a higher binding ability than that of the dextran conjugate as reported elsewhere (Ohyama et al., 1985).

3.2.2. Rearrangement of analytical components

Using the ligand conjugates and Con A as a binder, the glucose binding assay system can be constructed in various configurations (see Supplementary Fig. 2). As shown in Fig. 1, Con A can be immobilized on the sensor surfaces and the competition for Con A binding between the conjugate and glucose will occur (model A-1). Such restriction of Con A mobility is advantageous in two regards: suppression of multivalent binding ability and blocking potential toxicological effect on the body when the sensor is implanted. Alternatively, the two components can be arranged where the conjugate is on the solid surfaces and Con A is in the liquid phase (model B-1). Since the binder can interact with multiple ligands, this configuration could be used to increase the signal intensity from the sensor. In addition, cross-linking of both components could be used. Since both constituents displayed multivalency in regards to the binding reactions, one component can cross-react with the other component in the solid phase as well as in the liquid (models A-2 and B-2 corresponding to A-1 and B-1, respectively; see also Supplementary Fig. 2). Such an approach would amplify the signal. In overall, model A-1 was superior to the others in regards to the reaction rates on the sensor surfaces for complex formation and dissociation by competition. The baseline was also stable without drift, indicating a high reproducibility of the repetitive binding events. Therefore, configuration model A-1 was selected for further analysis since it could more accurately measure fluctuating glucose concentrations in the body.

It should be noted that, even for model A-1, the binding complex formation did not rapidly reach equilibrium, where the association and dissociation reaction rates were equal. We found that the background signal of the optical sensor without a ligand conjugate decreased in the presence of glucose and, in the absence of glucose, the background signal increased again (Fig. 2A). This up-and-down background pattern was highly reproducible; however, this was not observed when glucose in the medium was replaced with galactose. The negative control signal was also stable in the medium without a sugar component. Therefore, this background response may be specific to glucose binding to Con A immobilized on the sensor surfaces. The plant lectin, Con A, indeed undergoes a structural conformation change upon glucose binding to the pocket (Grimaldi and Sykes, 1975), which may vary the sensor surface occupancy of the protein and consequently alter the mean thickness of the molecular layer. Although this can be used as signal indicating the glucose concentration change in sample, it was not only slow in the dose response rate, but also relatively small in the intensity (refer to Fig. 2A, Glucose). To examine the net effect of this process, the glucose binding signal was subtracted from the mannose conjugate binding (2B, the upper panel), which allowed us to measure the differential signal (the lower panel). The net binding curve for the conjugate revealed that the response time for both of the association and dissociation by competition was less than 5 min. This symmetric response pattern of the sensor further demonstrates that the binding reaction between Con A and the ligand conjugate likely follows pseudo first-order kinetics.

3.2.3. Permeation of glucose across semi-permeable membrane

To continuously monitor the glucose concentration in vivo, the sensor compartment needs to be separated from the sample medium using a semi-permeable membrane (Fig. 3A). This would enable us to recycle the constituents of the sensor, which is important if this biosensor is to eventually be implanted inside the body. However, the membrane may act as a barrier against mass transfer of glucose into or out of the sensor compartment (Boss et al., 2011). Since the blood glucose concentration fluctuates rapidly upon food intake, the sensor should maintain a fast response time to changes in glucose concentrations. Therefore, it is crucial to choose a semi-permeable membrane that may not only hold the component, i.e., the ligand conjugate, within the sensing space, but also not limit the permeation rate of glucose across the membrane.

To select a membrane suitable for CGM, we tested polycarbonate membranes of different pore sizes (30–80 nm), and their performances in the glucose sensor were compared with that of regenerated cellulose, which is conventionally used for dialysis (Fig. 3B). The sensor was positioned in sequential sample wells containing 0 or 500 mg/dL glucose for 60 min each. The produced signals from Octet were recorded as a function of time using the program provided by the manufacturer, which were then normalized by aligning the signals detected at the initial time. This allowed us to compare the performances of the respective membrane in the association step (3B, the left), where the initial slope would reflect the efflux rate of glucose from the sensor compartment. The rate was directly proportional to the pore size of the polycarbonate membrane and their performances were superior to that of regenerated cellulose regardless of the pore size used. An appropriate pore size was determined to be 50 nm

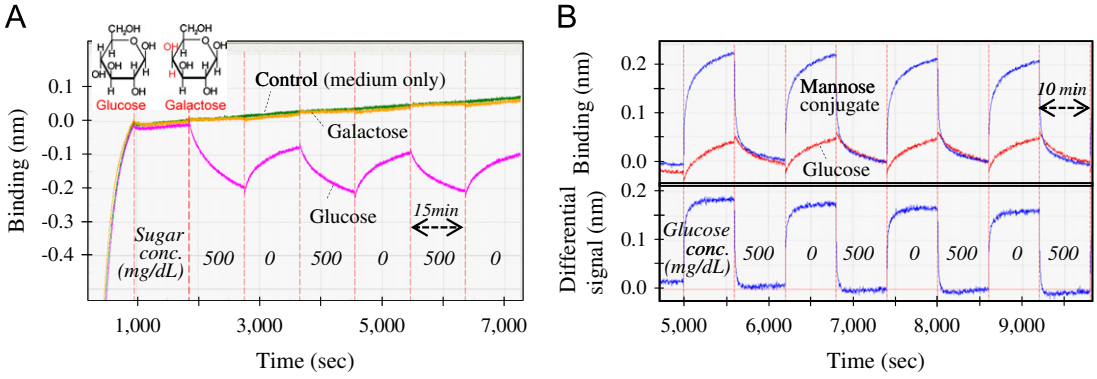

Fig. 2. Net effect of mannose-BSA conjugate binding to Con A. Con A was immobilized onto the sensor tip via biotin–streptavidin linkage between 0 and 900 s, which increased the signal in a sudden manner (A). When the sensor was then washed in a medium for the next 900 s, the signal was leveled off. Thereafter, for three cyclic dose changes of glucose or galactose in medium, the sensor responded to the glucose concentration changes while no response was observed in the presence of galactose. A negative control was also run in the absence of sugar (Control). The mannose-BSA conjugate binding subtracted from the glucose (B, the upper panel) demonstrated that the conjugate bound to Con A (the lower panel). (A) Glucose binding to Con A and (B) Net effect of conjugate binding.

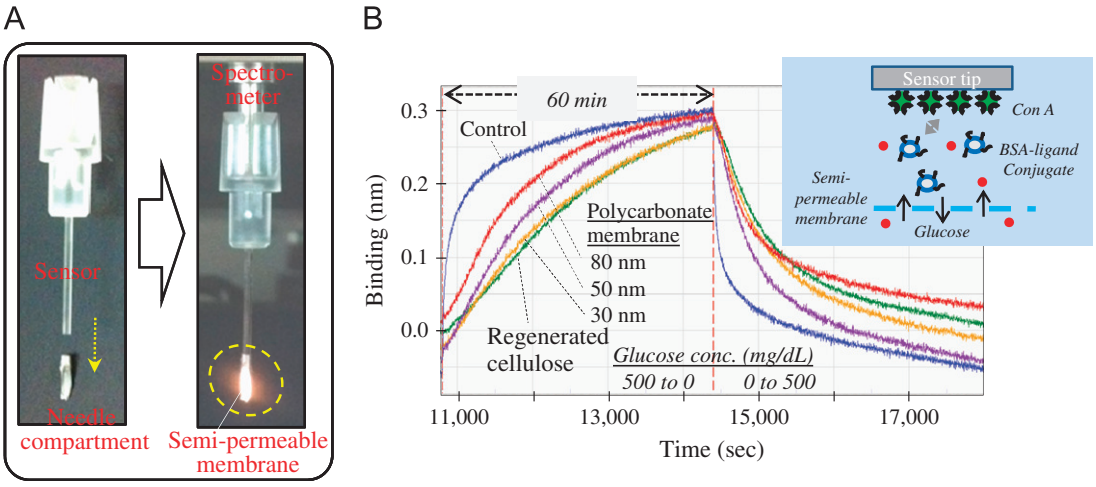

Fig. 3. Construction of a label-free sensor for CGM and comparison of the performances of different semi-permeable membranes installed in the sensor. Each glucose sensor was assembled using membranes with different pore sizes (A) and changes in the analyte concentration were measured with the different glucose sensors using Octet (B). The signals detected as a function of time were aligned at the beginning of the concentration change. This clearly separated the association curves (B, the left) in response to the dose decrease, and each slope indicated the efflux rate of glucose. The rate was proportional to the pore size of the polycarbonate membrane, all of which were faster than when regenerate cellulose was used. The binding curve without a membrane was also run as control. (A) Construction of needle–type glucose sensor and (B) Comparison of semi-permeable membrane performances.

when considering ligand retention inside the compartment (see below for further discussion). However, their responses were slow relatively to that of the control, which did not contain a semi-permeable membrane. These results indicated that an additional process aside from glucose permeation may still act as the rate-limiting step.

3.2.4. *Molecular diffusion of the ligand conjugate*

Due to the change in external glucose concentration, the competitive binding shown in Fig. 1 created a concentration gradient of the ligand conjugate between the solution and solid surfaces. This driving force resulted in mass transfer of the conjugate in either direction, depending on the glucose level. Since the internal medium of the sensor was stagnant and free of agitation, ligand only migrated through molecular diffusion (Boss et al., 2011). This process may control the overall performance of the sensor, particularly the response time, which could be varied by the molecular migration distance.

Although a 17 gauge (G) needle (see examples in Fig. 4A) was used during the initial study, a needle gauge with a smaller dimension, i.e., 19 G needle, could be used to decrease the diffusion distance. The internal diameter of this needle was just large enough to fit the Octet sensor, which allowed us to reduce the compartment volume by a 72%. The use of the 19 G needle also offered an additional benefit; the unnecessary volume present between the sensor and the internal wall of the needle was eliminated. To examine the effect of the needle size on sensor performance, sensors were constructed using the 17 G and 19 G needle and then the signals produced after incubation with glucose doses of 0 and 500 mg/dL for 30 min were measured (Fig. 4B). The sensor fabricated with the 19 G needle not only resulted in a significantly faster response than the 17 G needle, but also closely correlated with the time-response pattern of the control, which contained no membrane, after the glucose dose was changed. Furthermore, 12 repetitive measurements revealed that the ligand conjugate loaded in the sensor compartment was retained during the testing period when a semi-permeable membrane with a 50 nm pore size was used (4C). However, when an 80 nm-pore sized membrane was used, the maximum signal change at each cycle gradually decreased, indicating the components had leaked through the pores.

After subtracting the glucose binding effect on Octet (see Fig. 2B), we attempted to compare the response time of the test sensors. In practice, differential signals between the test sensor and control were measured so that the background effect could be canceled out (Fig. 4B, the inset). This approach enabled us to clearly show that the 19 G sensor reached final equilibrium in less than 15 min after the concentration change. On the other hand, the time required to reach equilibrium for the 17 G sensor was longer than 30 min. Therefore, under diffusion-limiting conditions, a reduction in the internal volume of the sensor significantly decreased the response time.

Indeed, the blood glucose concentration typically increases at a rate of 2 mg/dL/min upon dieting in diabetes patients (Dunn et al., 2004). The sensor response should not be slower than the relaxation time of the glucose concentration change so that no time lag can occur during CGM. The response time required under clinical conditions has been shown to be about 10 min (Boss et al., 2011), which is faster than that of the sensor shown in Fig. 4. However, further enhancements in the response time could be potentially attained by miniaturizing the needle dimension through the use of a smaller sensor although not commercially available to date.

3.3. *Dose responses to glucose concentration change*

To further test the performance of the glucose sensor, a needle-type biosensor was constructed and its ability to detect sequential, stepwise changes in glucose concentration was examined (Fig. 5). To this end, samples containing standard glucose concentrations were prepared in medium and placed in separate wells of a microtiter plate located within the Octet sensor system. The sensor was immersed serially in the respective wells maintained at 30 °C for 900 s each and the signals from the standard samples were recorded using the program (5A, Conjugate binding). The background was also monitored as described above using the same sensor except in the absence of the ligand conjugate within the needle compartment (Glucose binding). Differential signal was then calculated by subtracting the glucose binding signal from the conjugate binding signal (5B), which varied inversely with the glucose concentration in the external medium. The signals at each dose reached equilibria in less than 15 min, which closely mimicked the continuous monitoring of rapidly fluctuating glucose concentration. The signal at each dose

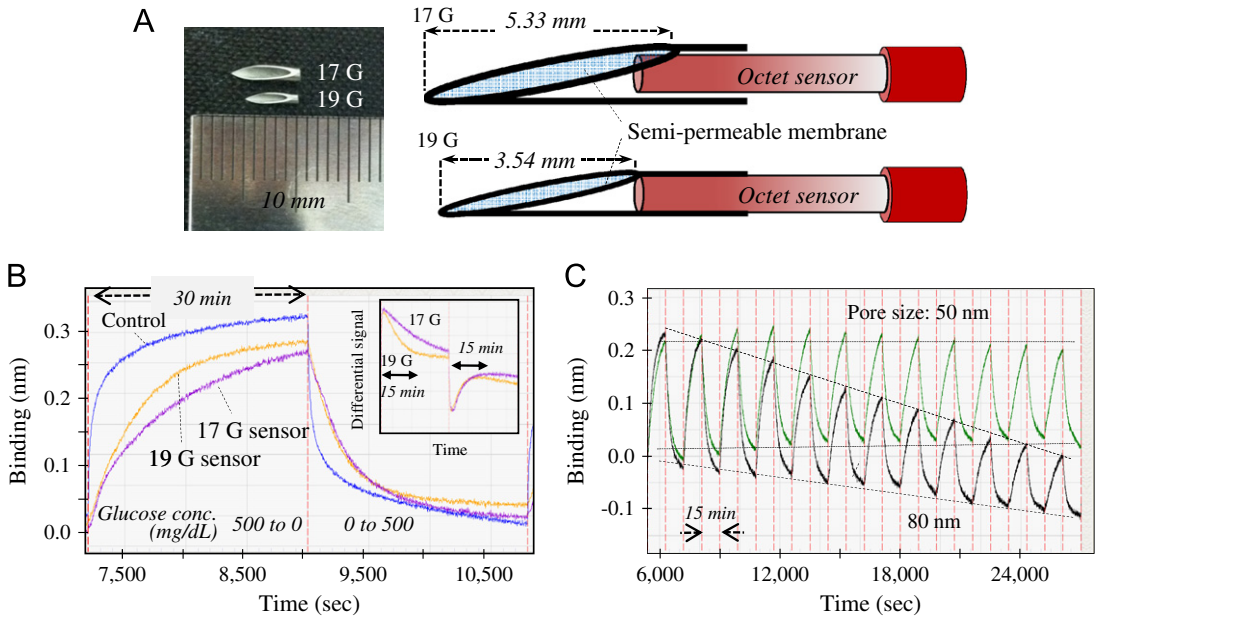

Fig. 4. Effect of internal volume of the sensor on the response time and retention of the ligand conjugate. Different sized syringe needles were employed to vary the sensor compartment dimension (A) and tested as potential factors controlling the response time (B). When the smaller 19 G needle was used, the response time was decreased. In addition, the ligand conjugate was retained when the membrane with a 50 nm pore size was used, while the ligand conjugate was lost when the membrane with a 80 nm pore size was used(C). (A) Needles available for glucose sensor, (B) Effect of internal volume of sensor and (C) Retention of ligand conjugate.

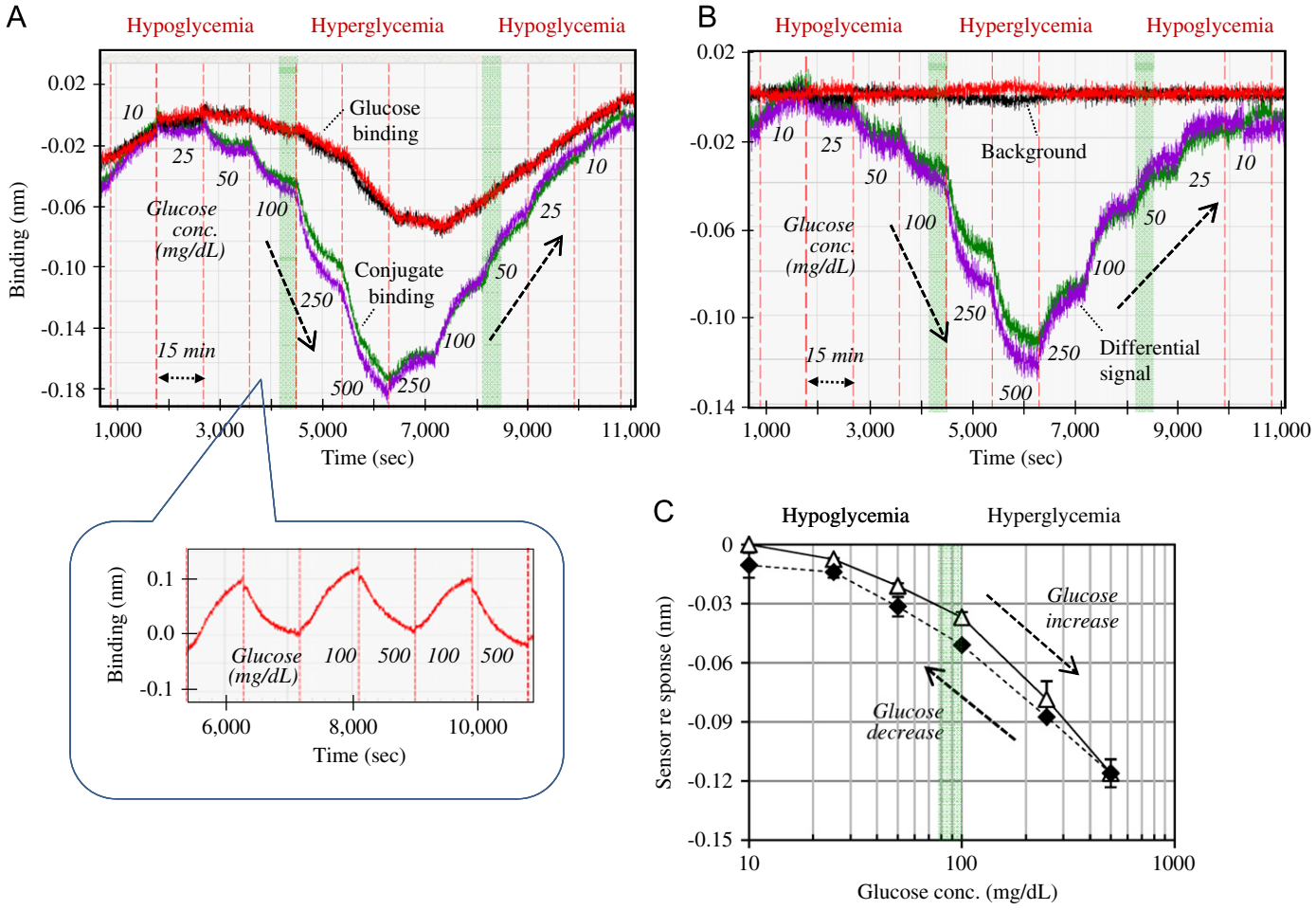

Fig. 5. Dose responses of the label-free, needle-type sensor to glucose in an external medium. The Octet sensor combined with the 19 G needle was fabricated under optimal conditions and used to monitor the stepwise change of glucose (10–500 mg/dL) in the external medium (A, Conjugate binding). In addition, the sensor without the ligand conjugate was also prepared to monitor the background (Glucose binding). The same sensor responses were obtained when glucose was added to human serum (the inset). The differential signal subtracted from the glucose binding signal was plotted against time (B). At each glucose dose, detection was conducted for 15 min, where the sensor signal was at equilibrium, which was then plotted against the glucose concentration (C). Variations of duplicate measurements at each dose were indicated in the plot. (A) Dose responses to glucose, (B) Dose responses based on differential signal and (C) Dose-response curve for 19G sensor.

was plotted against the analyte, which showed that the sensor could detect glucose over a wide dynamic range from 10 to 500 mg/dL (5C). The calibration chart indeed showed linearity in a clinical glucose concentration range between 50 and 500 mg/dL. Such performances were very close to those of the sensor system depending on viscosity change recently reported (Boss et al., 2011).

It should be noted that since the semi-permeable membrane used in the sensor had a pore size of 50 nm, certain glycoproteins in a real sample (e.g., serum) may be transferred into the internal compartment. However, an identical dose-response pattern to that demonstrated above was obtained using human serum as the sample medium (Fig. 5A, the inset). This indicated that the Con A-based competitive binding within the sensor was insensitive to the change of glycoprotein composition in the medium. Likewise, a ligand amount increase in the high concentration range (e.g., above 1 mg/mL) minimally altered the maximum signal level (refer to Supplementary Fig. 1B, Mannose conjugate). This signal, however, was rapidly inhibited when glucose was present in the sensor (see Fig. 2B), revealing that the glucose molecules in the clinical concentration range were much superior to the ligand in the competitive binding. Therefore, the ligand level insignificantly affects the sensor performances under the experimental conditions used.

It should be also notable that, in the cyclic dose responses of the sensor, the glucose binding signal was shown to follow a dose step behind the conjugate binding (see Fig. 5A). In particular, the conjugate signal was minimal at the highest glucose level and, on the other hand, the glucose signal was minimized at the next concentration in a delayed manner. This could be caused by a large difference in the Con A binding sites that can interact with each ligand species due to accessibility (Schramm and Paek, 1992). The binding sites accessible to a small molecule (e.g., glucose) would be much higher than those reactive with a large substance (e.g., mannose-protein conjugate). The sites not available for the conjugate binding could be hindered by the solid surfaces and also masked by protein molecules neighboring each other. Even for the glucose molecules, there might be a barrier against the accessibility to the net sites, which can also be postulated from the observation of the slow reaction rates in both of association and dissociation (see Fig. 2B, Glucose).

4. Conclusions

In the current study, the potentiality of using a label-free optical detection for CGM was demonstrated by applying the analytical concept proposed in Fig. 1 to the experimental model. The overall sensor response pattern was symmetric over a dynamic range, i.e., the increase and decrease in the signal according to glucose fluctuation was consistent. The dose-response curve showed a hysteresis effect, which resulted from a difference between the binding reaction kinetics of association of the ligand with Con A and dissociation from the binding complexes, depending on the direction of glucose concentration change. The performance of this sensor satisfied clinical needs regarding the rapid and continuous measurement of glucose over a wide dynamic range, which could be used for the smart delivery of insulin (Yin et al., 2010). The response time was less than 15 min even for serum samples and, according to the rate-limiting factor analyses, the response time could be further decreased down to about 5 min by decreasing the dimensions of the sensor. The bio-layer interferometric glucose sensor, to our best knowledge, is the first report that introduces the label-free optical biosensing for CGM with potential advantages: (1) no labeling needed, (2) transmission of optical signal without interference, and (3) suitability for highly abundant analyte. Furthermore, the needle-type sensor can be readily implantable in the body for true real-time monitoring of the blood glucose levels, provided the optical detector is developed on a small enough scale to be attached to the body.

Acknowledgments

This work was supported by the R&D Program of MKE/KEIT [10033747, Development of continuous glucose monitoring sensor for u-healthcare] and also by the National Research Foundation (NRF; Grant no. 20090083290).

Appendix A. Supporting information

Supplementary data associated with this article can be found in the online version at http://dx.doi.org/10.1016/j.bios.2012.05.038.

References

Boss, C., Meurville, E., Sallese, J.M., Ryser, P., 2011. Biosensors and Bioelectronics 30 (1), 223–228.
Chaudhary, A., Raina, M., Harma, H., Hanninen, P., McShane, M.J., Srivastava, R., 2009. Biotechnology and Bioengineering 104 (6), 1075–1085.
Dunn, T.C., Eastman, R.C., Tamada, J.A., 2004. Diabetes Care 27 (9), 2161–2165.
Grimaldi, J.J., Sykes, B.D., 1975. Journal of Biological Chemistry 250 (5), 1618–1624.
Hovorka, R., 2011. Nature Reviews Endocrinology 7 (7), 385–395.
Jin, S., Veetil, J.V., Garrett, J.R., Ye, K., 2011. Biosensors and Bioelectronics 26 (8), 3427–3431.
Krushinitskaya, O., Tønnessen, T.I., Jakobsen, H., Johannessen, E., 2011. Biosensors and Bioelectronics 28 (1), 195–203.
Leney, S.E., Tavaré, J.M., 2009. Journal of Endocrinology 203 (1), 1–18.
Li, S., Davis, E.N., Anderson, J., Lin, Q., Wang, Q., 2008. Biomacromolecules 10 (1), 113–118.
Liu, S., Weaver, J.V.M., Save, M., Armes, S.P., 2002. Langmuir 18 (22), 8350–8357.
Ma, C., Wang, A., 2010. Optics Letters 35 (12), 2043–2045.
Mandal, D.K., Kishore, N., Brewer, C.F., 1994. Biochemistry 33 (5), 1149–1156.
Mori, T., Toyoda, M., Ohtsuka, T., Okahata, Y., 2009. Analytical Biochemistry 395 (2), 211–216.
Ohyama, Y., Kasai, K., Nomoto, H., Inoue, Y., 1985. Journal of Biological Chemistry 260 (11), 6882–6887.
Paek, S.H., Cho, I.H., Seo, S.M., Kim, D.H., Paek, S.H., 2011. Analyst 136 (20), 4268–4276.
Schramm, W., Paek, S.H., 1992. Analytical Biochemistry 205, 47–56.
Steiner, M.S., Duerkop, A., Wolfbeis, O.S., 2011. Chemical Society Reviews 40 (9), 4805–4839.
Wang, J., 2007. Chemical Reviews 108 (2), 814–825.
Wei, C., Lunn, D.J., Acerini, C.L., Allen, J.M., Larsen, A.M., Wilinska, M.E., Dunger, D.B., Hovorka, R., 2010. Diabetic Medicine 27 (1), 117–122.
Yin, R., Han, J., Zhang, J., Nie, J., 2010. Colloids and Surfaces B 76 (2), 483–488.